energies

MDPI

Article

The Impact of Conventional Power Block Startup Procedures on the Fatigue Behavior of Drum Materials

Jerzy Okrajni [1,*], Krzysztof Wacławiak [1], Mariusz Twardawa [2] and Grzegorz Junak [1]

[1] Faculty of Materials Engineering, Silesian University of Technology, 44-100 Gliwice, Poland; krzysztof.waclawiak@polsl.pl (K.W.); grzegorz.junak@polsl.pl (G.J.)
[2] RAFAKO S.A., 47-100 Racibórz, Poland; mariusz.twardawa@rafako.com.pl
* Correspondence: jerzy.okrajni@polsl.pl

Abstract: Varying demands for electricity within the energy sector require the modification of operating modes to ensure both an uninterrupted electricity supply and the upholding of safety standards. This paper presents a method for the prediction of drum fatigue life, via the local analysis of stress–strain fields and low-cycle fatigue tests of the drum material. The analysis compares the fatigue properties of an unused material and a material that has undergone many years of operation. In addition, this paper suggests drum operating conditions based on the results of load testing under industrial conditions. The drum model was developed on the basis of technical documentation. The analysis includes the calculations of time-dependent temperature distributions, stresses, and strains for various drum startup modes. The drum material fatigue properties are determined under low-cycle conditions. Using the modeling results and fatigue properties, predictions of drum life for different startup modes are presented. The paper summarizes the impact of a range of startup procedures and the drum material fatigue properties on the fatigue life of a working drum, under various mechanical and thermal loads. In addition, this paper proposes a methodological approach to fatigue life assessment, as a combination of multiple research methods.

Keywords: power plants; drums; heat transfer; thermal stresses; thermo-mechanical fatigue; stress–strain behavior

Citation: Okrajni, J.; Wacławiak, K.; Twardawa, M.; Junak, G. The Impact of Conventional Power Block Startup Procedures on the Fatigue Behavior of Drum Materials. *Energies* **2022**, *15*, 3528. https://doi.org/10.3390/en15103528

Academic Editor: Jose A. Almendros-Ibanez

Received: 11 January 2022
Accepted: 9 May 2022
Published: 11 May 2022

1. Introduction

The power industry is facing new challenges, including the modification of conventional power generation devices for modern use. This requires traditional methods of fatigue life assessment to be revised. High-pressure boiler components operating in fossil fuel power stations must undergo such assessments. In particular, modernized blocks in coal-fired power plants must be adapted to operate with more frequent shutdowns and startups, and with an increase in the rate at which load parameters change under unsteady-state operating conditions. This requires an increased focus on the role played by both thermal stresses caused by non-uniform temperature fields, and fatigue processes in materials that are subjected to changing temperatures and the resulting thermal loads. Such conditions were not anticipated when existing blocks were designed, with loads expected to change much more slowly. Modern requirements necessitate that the energy generation capacity of plants must be flexible, in order to respond to demand in systems that feature both conventional power plants and renewable energy sources with variable efficiency. Previously, temporal variations in the temperature of power generation equipment were of lower importance. Devices intended for use in the transitional period between energy systems must be adapted to the new operating conditions. Increased requirements for the availability of units within energy systems necessitates operation under heavier loading conditions; such operation must ensure safe use and technical efficiency.

The power units in question vary in operational period and operating histories. An informed decision on the predicted operational capabilities of such units, and hence a deci-

sion on whether to upgrade or repair them to ensure safe operation requires an assessment of the current condition of the composite materials of the devices. The manner in which the changing operating conditions will affect strength characteristics and predicted durability must be determined.

For this reason, the characteristics of the units' load cycles are required. This includes the startup methods expected in given operating conditions, and an assessment of the impact of those conditions on time-varying stresses and strains in the power generation components under examination. From this, a prediction of component lifetime can be made. The inclusion of these data when predicting the strength of devices currently in use is important, both to ensure their safe operation and to determine the impact of the expected changes on the operating parameters of the devices. This paper studies power unit devices with capacities of 200 MW, which have been commonly used throughout the 20th and 21st centuries. Specifically, the boiler drums of such units are considered.

A detailed analysis is required to predict the time to crack formation on the surface of boiler drums, including the determination of temperature fields and stress and strain fields over the drum volume. Existing procedures to calculate the fatigue strength of pressure vessels use simplified dependencies. From these, stresses can be determined in addition to simplified fatigue characteristics in the form of S(N) curves, adopted according to the static tensile strength of the material in question [1]. The structural complexity of drums limits the measurement of the physical fields within them; modeling the behavior of such elements under operating conditions is the most convenient procedure for analyzing their structure and assessing durability. Reference sources on material fatigue include studies on the conditions of use for selected energy components under mechanical and thermal stresses, combined with the analysis of stress and strain states, which affect local fatigue damage accumulation processes [2–7].

To date, many papers have analyzed the mechanical properties of materials intended for high temperature applications. However, few publications have investigated the thermo-mechanical fatigue of devices under real operating conditions, where temperature fields are transient and material properties variable. One particularly relevant 2008 publication [8] summarized research conducted by a large 5th EU Framework Program: "Thermo-mechanical fatigue—the route to standardization", which concerned code-of-practice for strain-controlled thermo-mechanical fatigue testing. A survey of existing testing protocols and procedures was presented, and comprehensive pre-normative research activity into various issues was undertaken.

Hormozi et al. [9,10] studied steel failure under low cycle and thermo-mechanical tests, analyzing 316FR and 316 stainless steels. The authors attempt to describe failure mechanisms by linking experimental results with metallography analysis. In addition, creep-fatigue tests were conducted under both low-cycle fatigue and thermo-mechanical fatigue (TMF) conditions, with symmetrical hold time. The effects on microstructure were investigated using a scanning electron microscope. Following this, damage initiation was modeled using a hysteresis energy-based phenomenological approach. The authors developed a user-defined procedure that incorporating both the phenomenological approach and a creep damage approach using the time-fraction law.

Hyde et al. (2010) modeled material behavior under anisothermal conditions [11]. Isothermal fatigue tests were conducted to identify constitutive material parameters, using a modified Chaboche unified viscoplasticity model, which can handle isotropic and kinematic hardening, and rate-dependent effects associated with viscoplasticity. The experimental stress–strain characteristics of 316 austenitic stainless steel, in the form of hysteresis loops, were compared to modelling predictions. Amiable et al. (2006) discussed the results of thermal shock experiments [12]. Custom specimens made of 304L steel were continuously heated and cyclically cooled by focused water sprays. The temperature and stress fields were analyzed using the finite element method. The fatigue life criteria were analyzed and compared.

Pineau and Antolovich (2015) reviewed the micromechanisms of cyclic deformation, damage accumulation, and crack propagation in three types of material widely used in the power generation industry [13]. The properties of Cr–Mo steels, austenitic stainless steels, and super alloys used in jet engine turbines were analyzed. The creep-fatigue-oxidation behavior of such materials was particularly emphasized. Physical models of fatigue life prediction were examined, and the effect of hold time on the fatigue life of ferritic-martensitic, and austenitic steels was discussed in detail.

Ji et al. (2015) developed a novel creep-fatigue life prediction model, based on mechanical work density [14]. Experimental data were compared with predicted fatigue lifetimes and showed strong agreement. A probability analysis was presented and a reliability model was constructed.

Several works of Nagesha et al. are concerned with both the isothermal and thermo-mechanical fatigue of 9Cr–Mo ferritic–martensitic steels. Nagesha et al. [15] (2002) described the isothermal low cycle fatigue properties of one such steel within the range 300–873 K [16]. Nagesha et al. (2012) compared the results of two types of TMF tests—in-phase and out-of-phase—and isothermal low cycle fatigue tests, performed on 9Cr-Mo steel. The influence of variable temperature and load on the microstructure were described. The TMF tests were performed for different temperature ranges and for different total strain ranges. A comparison of the isothermal and TMF test results was discussed by Nagesha et al. (2013) [17].

Few investigations within the literature pertain to the thermo-mechanical fatigue of real devices operating in the power industry. Farragher et al. (2013) studied stress and strain fields in the headers and steam piping of power plants [2,4]. The authors attempted to assess and predict the life of such headers and piping via FEM simulations, based on material fatigue tests. They predicted the initiation of cracking on both the inside and outside of thick-walled components, with reference to cooling and heating transients.

Extensive research has been conducted on both thermo-mechanical fatigue and the relationship between fatigue and the creep phenomenon, in the structures of power boilers that operate under mechanical and thermal loading. Despite this, the evolution of damage within such devices is not well studied. Existing research has focused on the mechanical properties of the chosen materials and their operating or experimental conditions. Various durability criteria are used when both thermal and mechanical loading lead to the thermo-mechanical fatigue of vital infrastructure elements. In view of this gap in the literature, this work focuses on the highlighted problem, whether this concerns the material itself or the parameters of operation of the material. The outcome of this research should help to alleviate the uncertainty surrounding the decohesion of high-temperature-resistant materials, and provide insight into more sophisticated methods of durability assessment in the presence of both thermal and mechanical loads.

Few publications consider heat flow within the components of energy devices. Such heat flow determines the value of the accompanying time-dependent thermal stress [2–7]. A common approach is to use a constant heat transfer coefficient, to reflect the conditions occurring during heat flow through the considered elements [2–4,6,7]. Previous research has discussed the impact of this coefficient, and its time-dependency, on the course of temperature fields and related thermal stress distributions [18,19]. Using computational fluid dynamics, the heat transfer coefficient on the surface of selected components can be determined as a function of the time-varying parameters of the media flowing through those components, including the temperature and flow rate [5–7,18]. A number of studies have determined the heat transfer coefficient on the surface of components in which water, in either liquid or vapor form, is in contact with the metal [20–22]. However, only a small number of studies, such as [23], consider how this impacts the stress states and strength of the elements in question.

In particular, little attention has been afforded to the strength of boiler drums in the context of heat transfer phenomena, in addition to the fatigue processes that accompany startup and shutdown cycles. The studies that do concern boiler drum durability include those

investigating the impact of long-term operation on changes in the mechanical properties of drums—a relevant safety issue. Such studies include, among other directions, research on the structural changes within materials, and the subsequent effects on impact toughness under the influence of long-term operation [24–26]. In addition, analyses have been undertaken on the influence of power unit control strategies, intended to increase the availability of the corresponding power units as required by modern operating conditions [27]. Few articles, including [28], model stress states in drums under operating conditions.

To summarize, despite boiler drums performing essential roles within conventional power units, the available literature on durability and condition assessment methods for energy device components lacks strength analyses of drums. Existing studies focus primarily on the assessment of drum materials following long-term use. To the best of our knowledge, no studies adopt a methodical approach to strength analysis, with a particular emphasis on the relationship between heat flow and time-varying stress and strain distributions. These issues are of particular importance due to changes in the operating parameters of conventional power equipment—specifically operating cycle parameters. Such a detailed analysis is necessary to ensure the safe use of such devices in question. Furthermore, it will engender the development of guidelines for both the assessment of existing units following long-term operation, and the design of new pressure vessels with the use of computer modeling methods that account for complex geometric features and surface heat transfer conditions.

Via fatigue testing, this paper proposes a novel method for the durability assessment of boiler drums. An analysis is made based on the technical documentation of a selected drum, with measurements taken under operating conditions. The aim of this analysis is to determine the existing operating conditions—and predict the future state of such conditions—of similar devices, and to verify the accuracy of simulated parameters that determine the fatigue life of the tested pressure vessels. Additionally, this paper presents a method to predict the fatigue life of drums, based on both the local analysis of a stress and strain fields, and standard methods used by the designers of boiler drums. An example of fatigue life is presented, comparing an unused material with a material that has undergone extended operation.

To summarize, the analysis and discussion present the following contributions:

- The properties and operating conditions of the selected drum, based on the results of load testing under industrial conditions;
- The development of a drum model on the basis of the technical documentation, and the calculation of time-dependent temperature distributions and stresses and strains for various drum startup scenarios;
- Extensive material fatigue testing;
- a prediction of drum life for each startup cycle variant and varying fatigue properties of the material;
- a summary of the findings, including an assessment of the impact of startup procedures and material fatigue properties on the fatigue life of a drum subjected to variable mechanical and thermal loading.

Section 7 concludes the paper and presents methodological remarks resulting from the complementary nature of the research methods applied.

2. Thermo-Mechanical Loading of Boiler Drums

This paper studied a drum operating within a 200 MW power unit. Such drums are equipped with measuring systems that record the temperatures of water, steam, and metal at selected points via thermocouples. Moreover, parameters such as internal drum pressure and water level are measured during startup, steady operation, and shutdown of the block. These parameters are used in the process of controlling a power unit to ensure safe operation and assess performance. In addition, the measured values can be used to assess the time-varying mechanical and thermal loads that determine the time-dependent stress and strain distributions within the drum. Figure 1 shows a diagram of the drum, with the

thermocouple locations indicated. Along the horizontal axis, the thermocouples are located on the left, middle, and right of the drum. Along the vertical axis, the thermocouples are located at the top and bottom of the drum. At each location, both deep and medium-deep thermocouples are attached, relative to the outer surface of the drum. Medium-deep thermocouples are positioned equidistant from the internal and external drum walls; deep thermocouples are positioned 5 mm from the internal wall, exposed to water or steam.

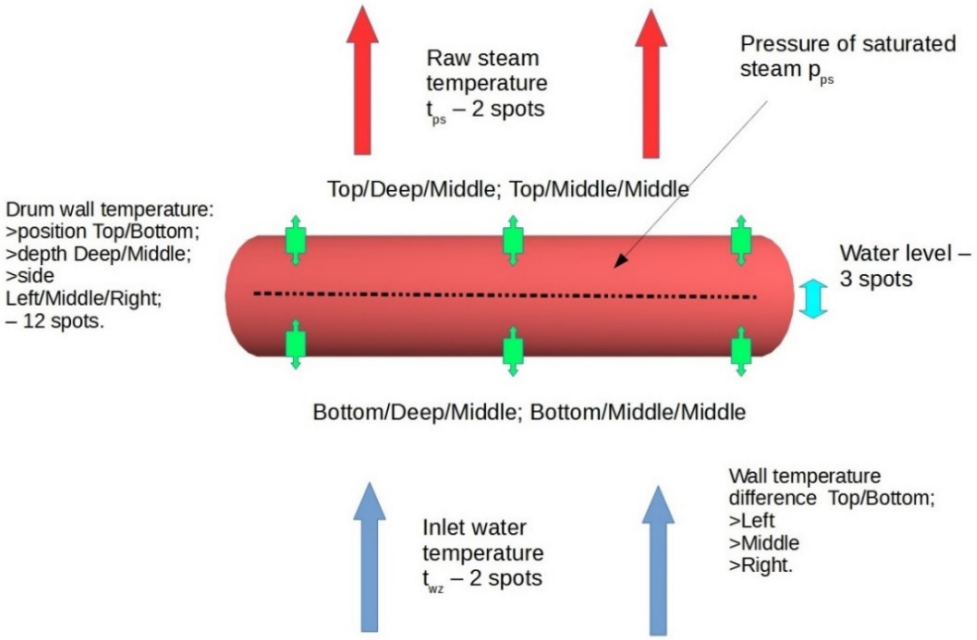

Figure 1. Schematic diagram of the temperature and pressure measuring systems of a boiler drum, with thermocouple locations indicated.

Figure 2 shows the time-dependent progression of the steam temperature and pressure for two scenarios: cold startup and hot startup. This distinction is made by differing initial temperatures and rates of change of the steam temperature and pressure.

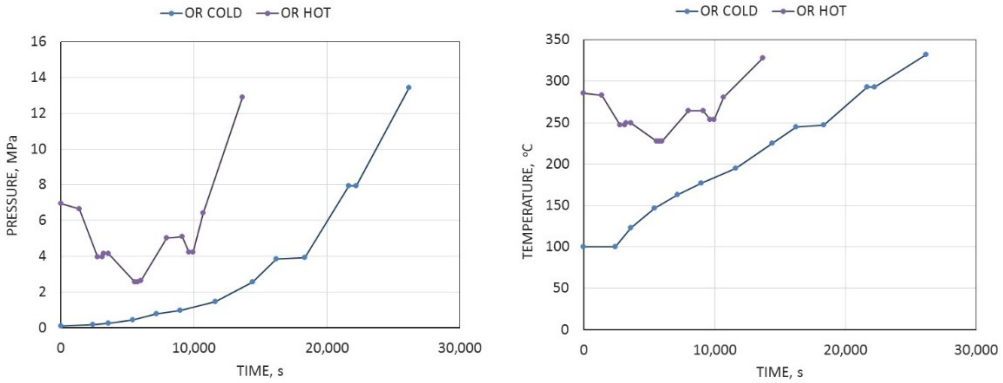

(**a**) (**b**)

Figure 2. Changes in (**a**) steam pressure and (**b**) temperature within a drum under cold startup operation (OR COLD) and hot startup operation (OR HOT), when subjected to real industrial conditions.

Cold startup conditions with different rates of change of steam temperature were also considered. The characteristic mechanical and thermal loads for these scenarios are presented in Figure 3.

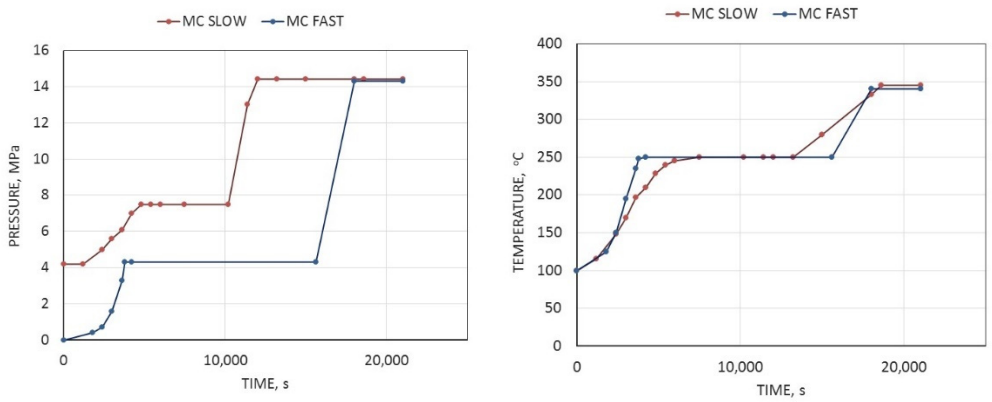

(**a**) (**b**)

Figure 3. Changes in (**a**) steam pressure and (**b**) temperature within a drum under cold startup operation with lower (MC SLOW) and higher (MC FAST) rates of change of steam temperature.

Henceforth, the scenarios presented in Figures 2 and 3 are referred to as:

- OR COLD, a cold startup under real operating conditions;
- OR HOT, a hot startup under real operating conditions;
- MC SLOW, a model cold startup with a lower rate of change of steam temperature;
- MC FAST, a model cold startup with a higher rate of change of steam temperature.

3. Boiler Drum Model

Figure 4 presents the 3D boiler drum model, featuring the shell, the undercarriage, and the connected pipe nozzles. The model was developed using the engineering simulation software ANSYS.

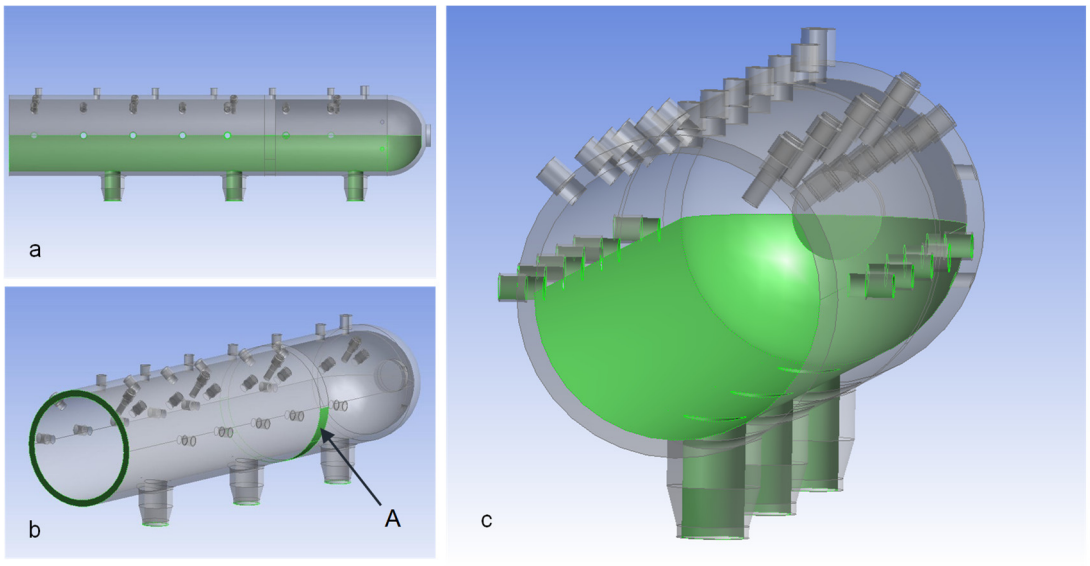

Figure 4. Multiple perspectives of the 3D drum model. Front view of the right part of the drum with the water level marked (**a**). Perspective view with the plane of symmetry in the cross-section and the area of influence of the suspensions marked with the letter A (**b**). Perspective view from the left front side of the drum (**c**).

Figure 4 presents selected views of the model. The model components were made transparent so as to show all details. Simplified representations of the drum shell, undercarriage, manhole, and the stub pipes connected to the drum shell were all visible.

Due to the symmetrical shape of the drum, only the right half was shown. In Figure 4a,c, contact between the internal surface and the water is marked in green. The remainder of the internal surface and the nozzles are in contact with water vapor.

In Figure 4b, green regions, which correspond approximately to the suspension points, are those for which displacement limitations were assumed. The geometric features determine the boundary conditions in calculations of the heat flow and the stress–strain field calculations. A displacement of zero was assumed across the cross-section of the drum perpendicular to the drum axis. The model featured flexible supports of the downpipe nozzles and the areas at the left and right ends of the drum, where the hangers on which the tank is suspended are in contact with its lower external surface. The hangers were composed of links connected by articulated joints made of steel sheets and flexible spacers. As shown in Figure 4b, the contact area between the hangers and the external surface of the drum is marked in green and indicated by 'A', at the end of the right half of the drum.

This model was developed on the basis of schematics provided in the technical documentation. In the calculations below, heat exchange on the internal surface of the drum was assumed to differ for the areas of the surface exposed to water and those exposed to steam.

The physical properties of the drum material, 15NCuMNb steel, which are required for the computation of the time-varying temperature fields, were calculated by the Institute for Ferrous Metallurgy in Gliwice, Poland [29].

To analyze the stress and strain fields, a multilinear kinematic hardening model was adopted, as proposed by Besseling [30–32]. The model assumes that the elementary volume of an elastic-plastic material can be treated as multiple sub-volumes, which share the same modulus of elasticity and undergo the same deformation, but have different yield limits. Each such sub-volume is assumed to exhibit ideal plasticity. When considered as a whole, the set of sub-volumes can describe complex behavior, represented by a broken strain curve that exhibits a Bauschinger effect. The volume fraction (weighting factor) and the yield point for each sub-volume are defined by fitting the material response to either the cyclic hardening curve, or a curve determined by uniaxial tensile testing.

This is a standard material model used by the ANSYS software. Dependent on the temperature, the cyclic stress–plastic strain curves and the Young's modulus are taken as characteristic of the material behavior. Examples are shown in Section 4.2. These calculations use a cyclic stress–plastic strain curve model determined for the material after long-term operation at both room temperature and at 623 K. A linear approximation was used to define the curves for the remaining temperatures.

4. Temperature and Stress and Strain Calculations for Various Boiler Drum Startup Scenarios

4.1. Thermal Analysis

For the initial temperature field calculations, the heat transfer coefficients were taken from the PN-EN 12952-3 pressure vessel design standards. The assumed coefficients for water and steam were 3000 W/(m^{2}K), and 1000 W/(m^{2}K), respectively. The heat transfer coefficient of the external surface was assumed to be 40 W/(m^{2}K), and the environmental temperature in the vicinity of the drum was taken to be 313 K. Following the initial calculations, the boundary conditions were modified to improve the accuracy of the calculated results when compared to experimental measurements. The modified calculations used coefficients of 4500 W/(m^{2}K) and 2000 W/(m^{2}K) for water and steam, respectively. The heat transfer coefficient of the external surface was assumed to be 10 W/(m^{2}K), and the environmental temperature in the vicinity of the drum was taken to be 313 K. The changes in the time-dependent mechanical loading and temperature, which were used as boundary conditions, are presented in Figures 2 and 3.

The time-dependent temperature fields were obtained for the drum. Figure 5 shows examples of the field distributions at selected times, and Figure 6 demonstrates the temperature changes at selected points on the drum. The time-dependent temperature changes are taken from locations both along the internal surface and beneath it, equidistant between the

internal and external surfaces. These locations correlate approximately with the deep and medium-deep measurements, in the upper-center and lower-center sections of the drum. Figure 5 shows the temperature distributions for the internal and external surfaces of the drum, and across the planar cross-section, at selected times during hot startup.

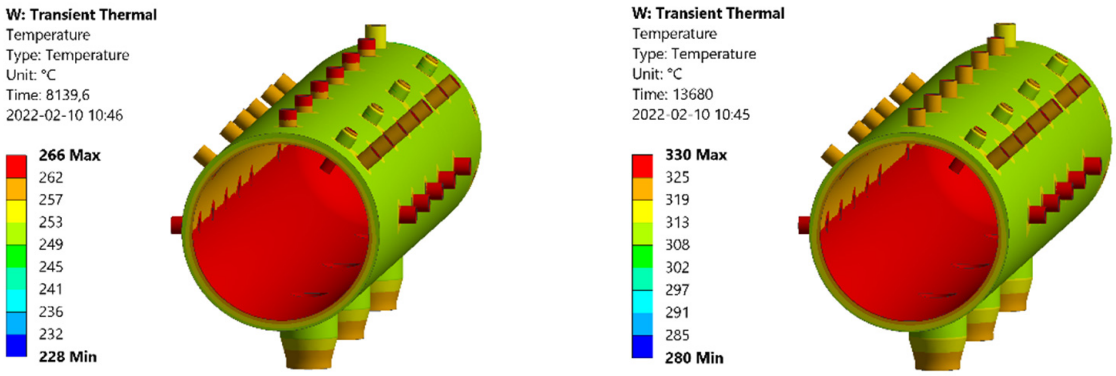

(**a**) (**b**)

Figure 5. Examples of temperature distribution on the internal and external drum surfaces, and across the planar cross-section, at (**a**) 8140 s into the OR HOT start cycle, and (**b**) at 13,680 s into the OR HOT start cycle.

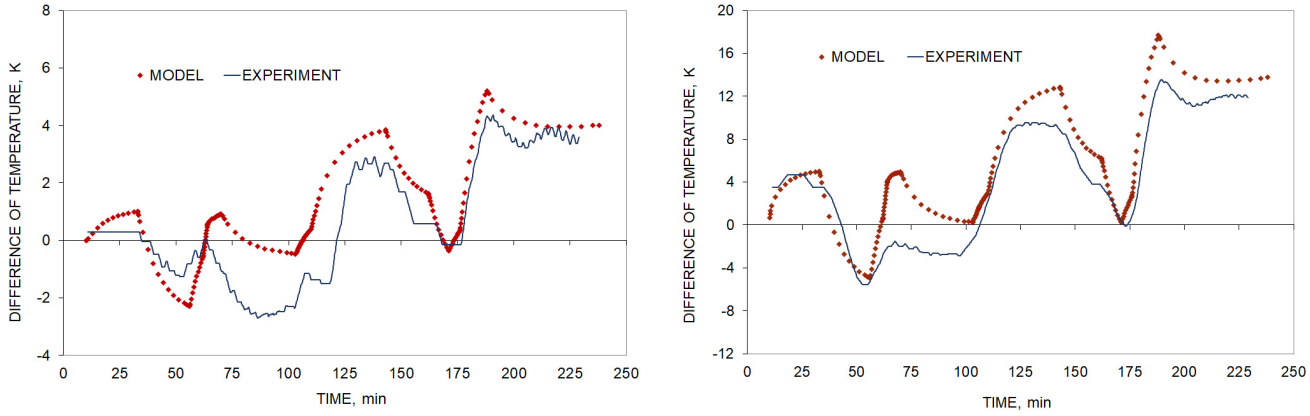

(**a**) (**b**)

Figure 6. Comparison of the calculated and measured temperature differences for medium-deep and deep points at the (**a**) top middle and (**b**) bottom middle of the drum, during an OR HOT start cycle.

The graphs shown in Figure 6 compare the calculated (red) and measured (blue) temperature changes during hot startup at the deep and medium-deep measurement points at the top and bottom of the drum, midway along its length. The discrepancies between the measured and calculated values result from the archiving software used in the power plant IT system. The software stores the last value recorded until a newly recorded temperature exceeds the current stored value within a margin of change. Thus, the time-dependent temperature changes are shown as step curves. Due to the time lag between the individual thermocouples, subtracting the temperature values presented in this way results in the waveforms shown in Figure 6.

Such discrepancies could also be attributed to the adopted values of the heat transfer coefficients. Previous research [33,34] has shown that the accuracy of temperature field models can be improved by adjusting the values of the coefficients to match selected

experimental data. To this end, the boundary conditions were adapted in accordance with the standards, as described above.

The changes in external load and temperature for the OR HOT startup are shown in Figure 2. Henceforth, calculations are made using the modified boundary conditions.

The impact of startup parameters on the changes in temperature fields within the drum and the related thermal stresses was assessed based on the discrepancies in temperature changes throughout the drum. For example, temperature differences between the internal surface and a point close to the external surface were considered. Temperature variations on the internal and external surfaces could indicate an uneven distribution within the drum wall, and affect the thermal stresses caused by changes in water and steam temperatures during unsteady state operation of the boiler.

Figure 7 shows the time-dependent temperature changes for the considered startup scenarios. The MC FAST rapid cold-state startup displays the highest temperature differences. This indicates increased thermal stresses in this startup scenario. Note that thermal loads are accompanied by mechanical loads, primarily pressure and weight, whose combined effects were considered in the mechanical analysis.

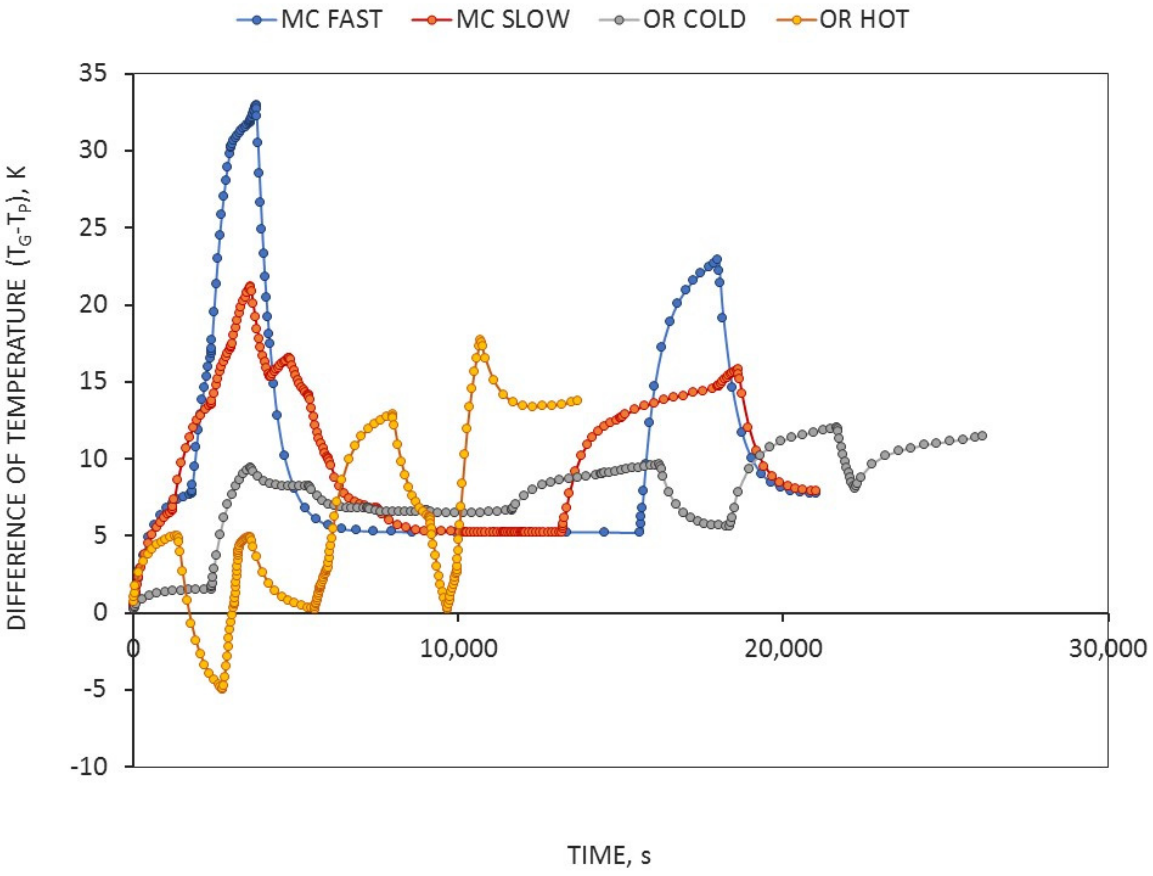

Figure 7. Time-dependent temperature differences between the internal and external surfaces at the middle bottom of the boiler drum for the considered startup scenarios.

4.2. Mechanical Analysis

The time-dependent stress and strain components were calculated for the OR COLD, OR HOT, MC SLOW, and MC FAST startup scenarios. Determined from the multilinear kinematic hardening model, Figure 8 presents the temperature-dependent Young's modulus, and cyclic stress–plastic strain curves at both room and elevated temperatures.

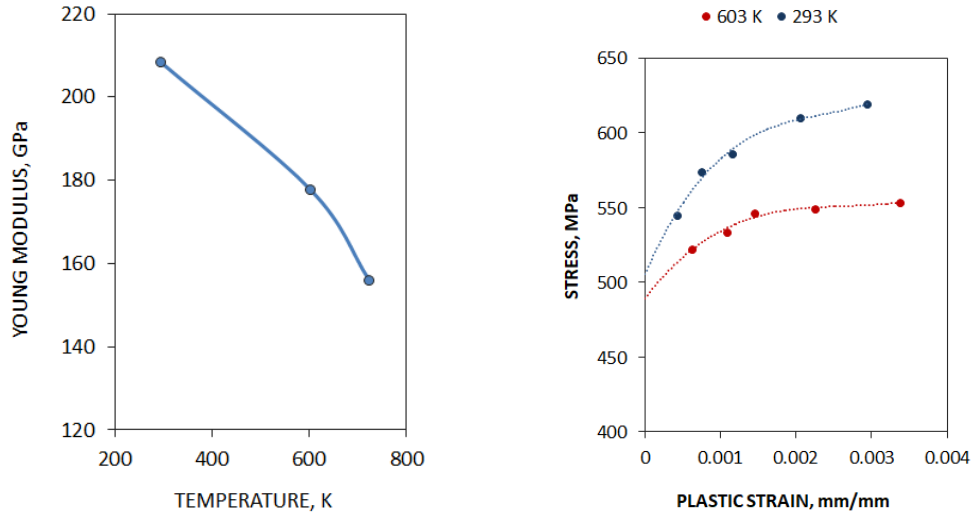

(**a**) (**b**)

Figure 8. Mechanical parameters of 15NCuMNb steel following 250,000 h of operation, determined from the multilinear kinematic hardening model. (**a**) Temperature-dependent Young's modulus and (**b**) cyclic stress–plastic strain curves at 293 K and 603 K.

Figure 9 illustrates the results of the selected stress and strain calculations. Stress accumulation areas are marked in red. These areas were predicted to accumulate substantial fatigue damage when subjected to frequent startups.

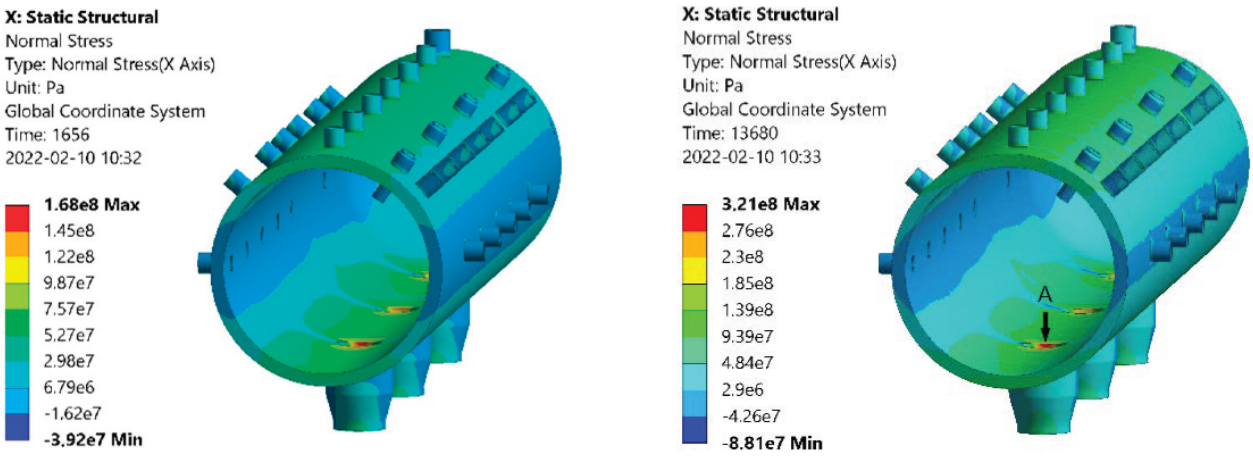

(**a**) (**b**)

Figure 9. Examples of σ_x component stress distributions on the internal and external surfaces of the drum, and on the planar cross-section, at (**a**) 1656 s into the OR HOT startup OR HOT, and (**b**) 13,680 s into OR HOT startup.

The time-dependent stress and strain changes were determined at point A, as indicated on Figure 9b. This point is located on the edge of the downpipe in the area with the highest stress. Stress versus strain characteristics were also determined at this point. Figures 10–13 present circumferential stress and strain results for points along the edges of the downpipe spouts, where the hoop stresses reached the highest values. Such hoop stresses are important criteria for the assessment of pressure vessel fatigue life [1].

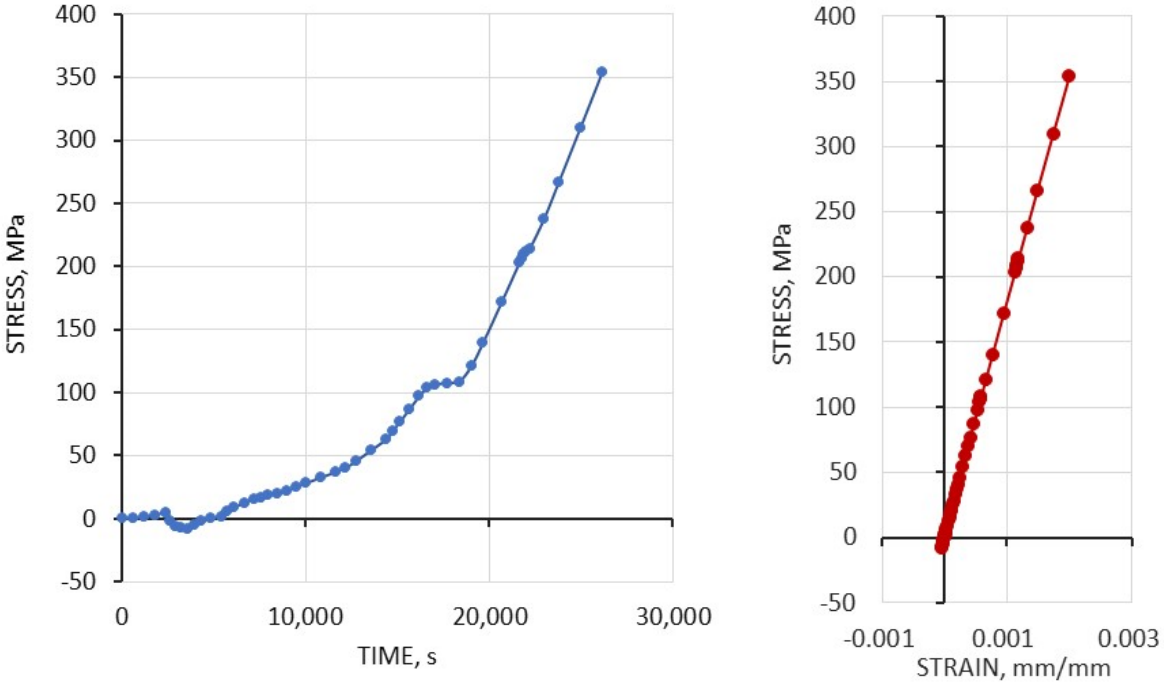

(**a**) (**b**)

Figure 10. The (**a**) time versus stress and (**b**) stress versus strain relationships in the OR COLD startup scenario, under industrial operating conditions.

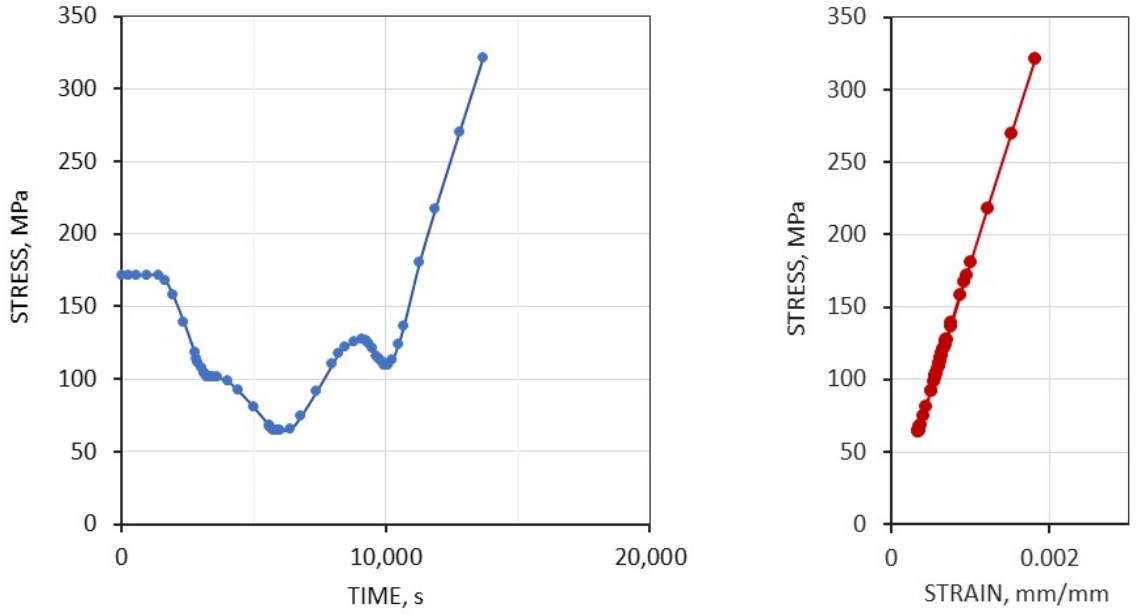

(**a**) (**b**)

Figure 11. The (**a**) stress versus time and (**b**) stress versus strain relationships in the OR HOT startup scenario under industrial operating conditions.

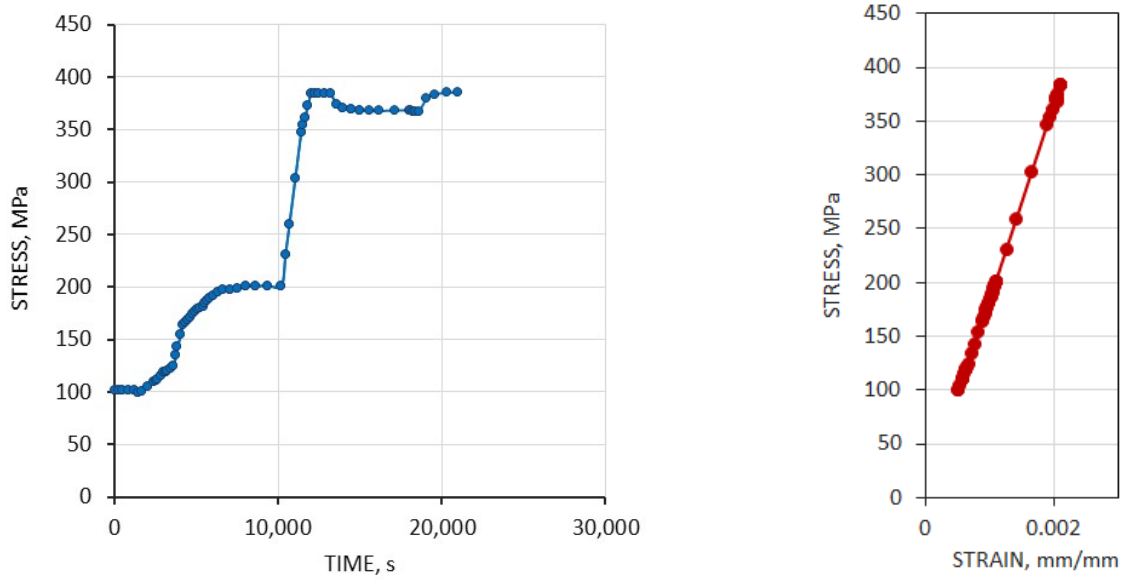

Figure 12. The (**a**) stress versus time and (**b**) stress versus strain relationships for the MC SLOW cold startup computational model, with a decreased rate of change of steam temperature.

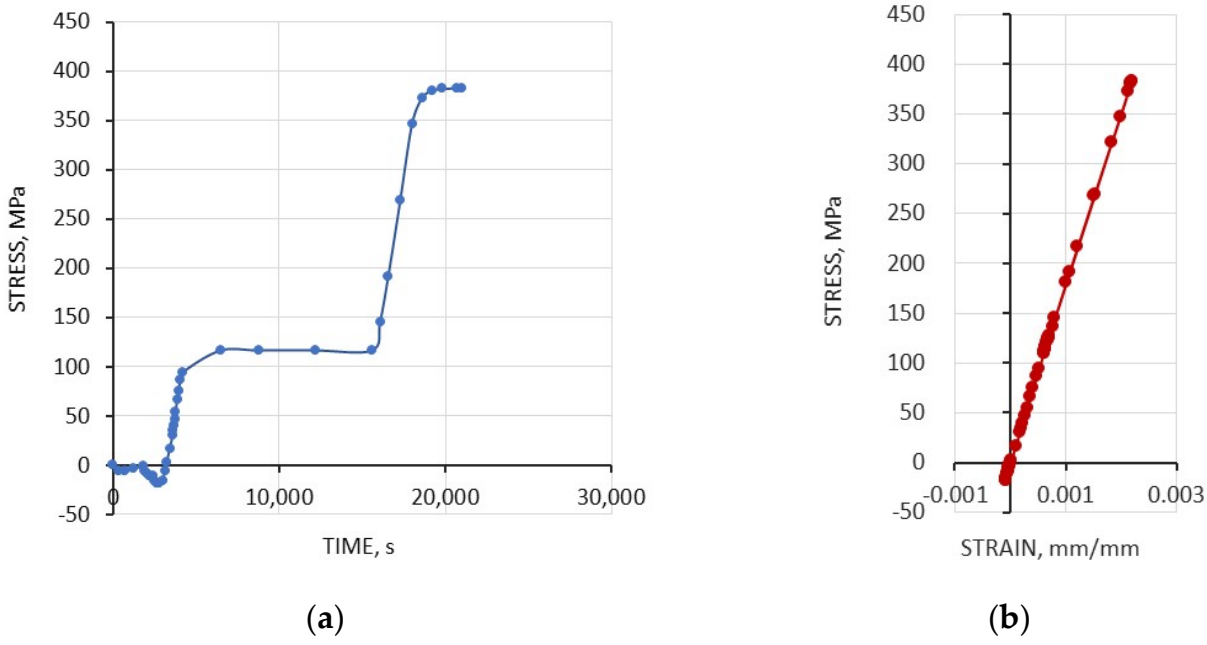

Figure 13. The (**a**) stress versus time and (**b**) stress versus strain relationships for the MC FAST cold startup computational model, with an increased rate of change of steam temperature.

The stress and strain component relationships were used to assess the range of changes in these values, and compare them with the fatigue characteristics determined from the fatigue tests. Using these data, the fatigue life could be estimated. Calculations presented in the following sections of this paper form a comparison of the different startup procedures, accounting for their impact on the intensity of damage accumulation in the previously defined areas.

5. Material Fatigue Tests

Fatigue life can be considered as the number of cycles until cracks appear in the spout openings. Fatigue tests of 15NCuMNb steel were performed using an MTS servo-hydraulic system, which was equipped with a subsystem for heating specimens by induction. Fatigue tests were conducted on both used and unused samples. The used samples were taken from drums that had undergone 250,000 h of operation. The unused samples were taken from new material, in the form of 100 mm thick metal sheet. A durability criterion was required that would be sufficiently universal for a range of materials subjected to fatigue in isothermal conditions, and the temperature changes that accompany stress and strain variations. The Ostergren criterion [2,4,35,36] is commonly used, and includes two parameters that are dependent on fatigue conditions, the plastic strain range and the maximum tensile stress when subject to cyclic load and temperature changes. The effect of temperature on fatigue life is considered indirectly by its impact on the above parameters.

Additional criteria were considered, such as one that incorporated the total strain range and stress range, in addition to the maximum temperature during load cycling. The criterion characterizes the number of cycles until failure for a specimen under isothermal testing conditions and takes the form $P = \Delta\varepsilon_p \cdot \sigma_{max} \cdot T_{max}$ [37], where $\Delta\varepsilon_p$ is the range of plastic strain, σ_{max} is the maximum mechanical or thermal stress during the loading cycle, and T_{max} is the maximum temperature during the test. The usefulness of such a relationship for the assessment of durability of structural parts under thermal and mechanical load is the subject of our ongoing research. Although preliminary studies have produced promising results, for the current study, we opted to use proven methods of fatigue life estimation. The chosen method was the procedure described in [1].

Table 1 shows the results of low-cycle isothermal fatigue tests.

Table 1. Summary of the fatigue test results.

T, K	$\Delta\varepsilon_c$	$\Delta\sigma$, MPa	$\Delta\varepsilon_s$	$\Delta\varepsilon_p$	σ_{max}, MPa	N_f
Before Operation						
293	0.006	911	0.004370	0.001630	455	7850
293	0.007	947	0.004546	0.002454	474	4938
293	0.008	964	0.004626	0.003374	482	3158
293	0.01	1006	0.004827	0.005173	503	1704
293	0.012	1034	0.004962	0.007038	517	1158
603	0.006	1040	0.005856	0.000144	520	1862
603	0.007	1141	0.006425	0.000575	570	1279
603	0.008	1135	0.006390	0.001610	567	798
603	0.01	1165	0.006558	0.003442	582	626
603	0.012	1218	0.006857	0.005143	609	378
After Operation						
293	0.006	1090	0.005149	0.000851	545	2386
293	0.007	1147	0.005420	0.001580	573	1452
293	0.008	1173	0.005540	0.002460	586	1165
293	0.01	1220	0.005765	0.004235	610	764
293	0.012	1239	0.005851	0.006149	619	358
603	0.007	1067	0.006289	0.000711	534	1236
603	0.008	1093	0.006441	0.001559	547	1087
603	0.01	1099	0.006475	0.003525	549	630
603	0.012	1107	0.006524	0.005476	554	260

Figure 14 presents fatigue curves derived from these data for the used (AO) and unused (WO) specimens. The graphs show the number of cycles to failure versus the total strain range at both room temperature and 603 K temperatures. The fatigue test results were approximated by a power law function.

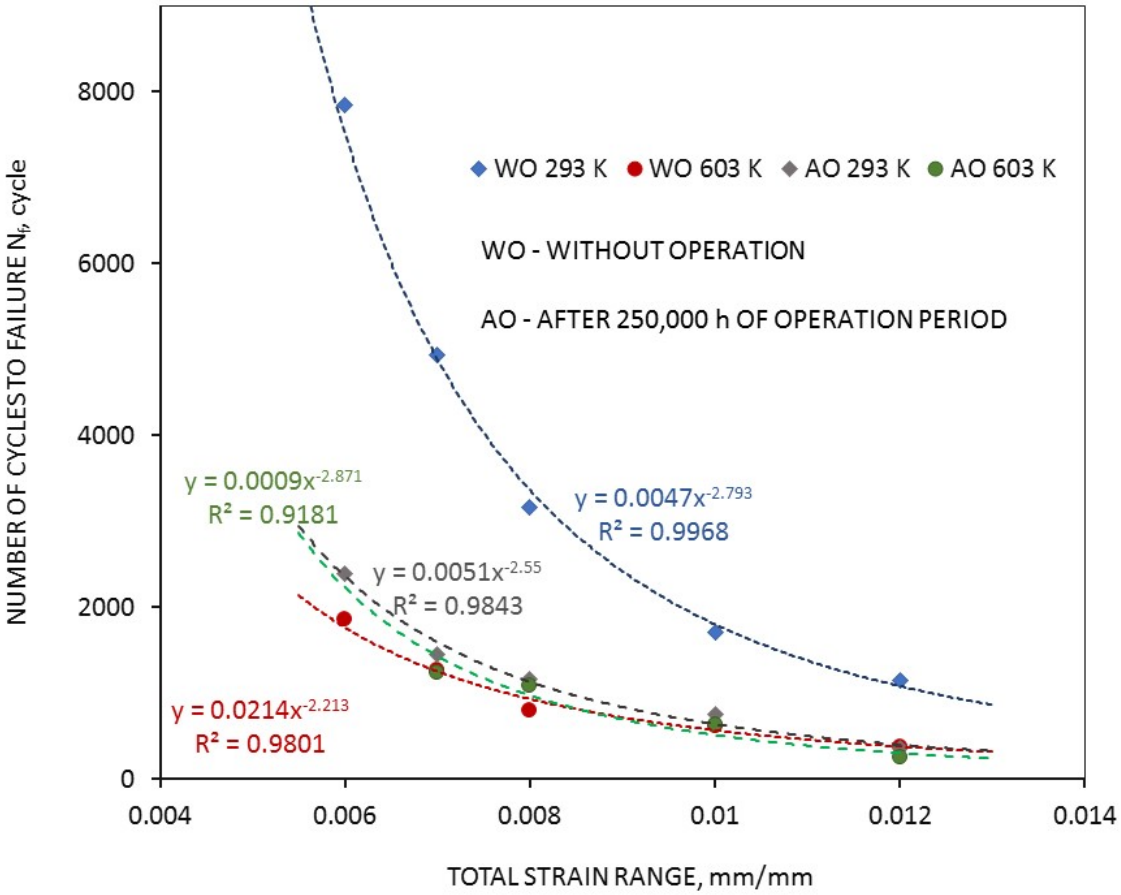

Figure 14. Fatigue curves of the number of cycles to failure (N_f in Table 1) versus total strain range ($\Delta\varepsilon_c$), for the entire population of materials tested.

Substantial differences can be observed between the WO and AO samples both at room temperature and 603 K. The WO sample displays a substantial decrease in the number of cycles to failure as the temperature decreases. However, the influence of temperature on the AO sample is negligible, with the number of cycles to failure being almost identical at both temperatures. The WO sample at 603 K displays very similar behavior to the AO sample at both 603 K and room temperature. The justification for this key observation requires that the structural changes of the material be investigated via electron microscopy methods. This is particularly applicable to the dislocation structure of steel: extended operation at elevated temperature favors dislocation movements leading to the stabilization of the mechanical properties. Such studies are planned for future stages of the work.

6. Discussion and Findings

The majority of the material condition assessments for components operating at elevated temperatures for extended periods of time focus on creep analysis. Such an approach is appropriate for components subjected to substantial material changes under long-term loading conditions, which includes most components of energy boilers. However, as the necessity of frequent startups increases, due to the changing demand for electricity, the analysis of materials subjected to varying loads becomes more important. As such, the requirement for monitoring fatigue processes is increasing, and fatigue testing must

become part of the standard assessment procedures of power unit components approved for operation. Boiler drums in conventional power units are particularly vulnerable to fatigue.

Current knowledge of the changes caused to materials by prolonged operation is limited, and methods for forecasting the fatigue life of components are imperfect. As such, assessments of fatigue damage probability may be inaccurate. To improve fatigue assessments, further investigation is required into durability estimation under various operating conditions and a range of management and operational practices. This paper sought to address this key issue.

The conclusions of Section 5 compare the fatigue behavior, at different temperatures, of new material and material that has undergone extended operation. The primary analytical focus was on the startup scenario, because changing startup procedures is the only practical method to increase boiler flexibility. Therefore, current boiler design standards were implemented to link numerical modelling with industrial measurements and determine the modelling parameters [1].

This study assessed fatigue damage accumulation near the edges of the drum downpipe inlets, where areas of high stress accumulation were detected. A high focus was placed on the hoop stresses within the drum, the importance of which are emphasized by the life expectancy calculation standard EN 12952-3 [1].

The aforementioned design standard [1] for pressurized boiler components makes use of an equivalent local range of stress, referred to as $2f^*_a$. Accounting for both this quantity and a safety factor, the number of cycles to failure can be estimated via diagrams or numerical relationships.

Such diagrams and relationships are correlated with the tensile strength of materials. A new quantity $2f_{av}$ (Table 2) is determined as the range of change between principal stress differences at a chosen point $\sigma_{max}-\sigma_{min}$. In addition, f_v is defined as the mean value of the principal stress differences at the chosen point. Both $2f_{va}$ and f_v are multiplied by corrective coefficients, that are functions of surface quality and weld type, to determine the corrected quantities $2f^*_{va}$ and f^*_v. Two safety factors are implemented: one refers to stresses and the other to loading cycles. The former is set to 1.5, and on multiplication by $2f^*_a$ gives $2f_{as} = 2f^*_a \cdot 1.5$, on which depends the number of cycles to failure N_{AS}. The latter safety factor is assumed to be equal to 10, and a new quantity N_{AL} is determined by dividing the lifetime determined for $2f^*_a = 2f_{aL}$ by 10. The smaller of N_{AS} and N_{AL} is referred to as the fatigue lifetime limit. Table 1 presents N_{AS} and N_{AL} values, calculated by the above method. Table 1 also shows the tensile strength of the analyzed steel grade. The yield stress of the material at an equivalent temperature, defined by the design standard, was assumed to be 460 MPa. The value of the surface quality and weld type corrective coefficient was assumed to be 3.5. The results of the durability assessment calculations for each of the analyzed startups are presented in Figures 15 and 16.

Table 2. Summary of the fatigue life calculations.

	$2f_{va}$, MPa	f_v, MPa	$2f^*_{va}$, MPa	f^*_v, MPa	R_m, MPa	$2f^*_a$, MPa	N_{AS}, Cycle	N_{AL}, Cycle	$N_{AL}/N_{ALORCOLD}$
OR COLD	363	186	1271	649	679	1755	3198	866	1.00
OR HOT	268	200	938	700	679	957	15,131	6164	4.73
MC SLOW	293	251	1027	877	679	1146	9147	3103	2.86
MC FAST	383	206	1342	719	679	1957	2495	653	0.78

The results presented in this paper show that the number of cycles to failure, as estimated by two different safety factors, produce two different fatigue life values. The value based on the number of cycles to failure, S_L, is lower than the value based on the defined stress level, S_S. As such, the number of cycles to failure N_{AL}, presented in Table 1, is taken as the final estimated fatigue life of the analyzed material. Using this value, diagrams were produced for both absolute fatigue life and fatigue life relative to the current startup

procedure. The relationships between startup scenario and fatigue life were presented in this manner.

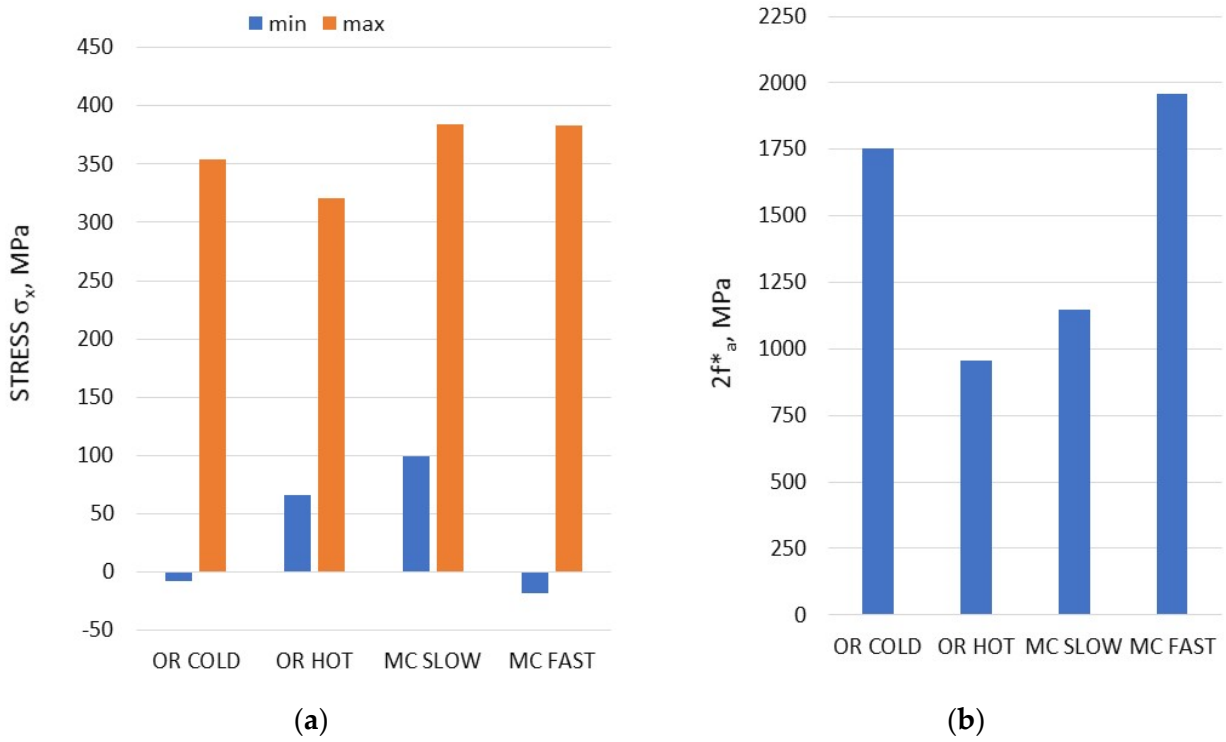

(**a**) (**b**)

Figure 15. Stress components σ_{xmax} and σ_{xmin} for each startup scenario: (**a**) the stress cycle at point A and (**b**) the equivalent local range of stresses $2f^*_{a.}$

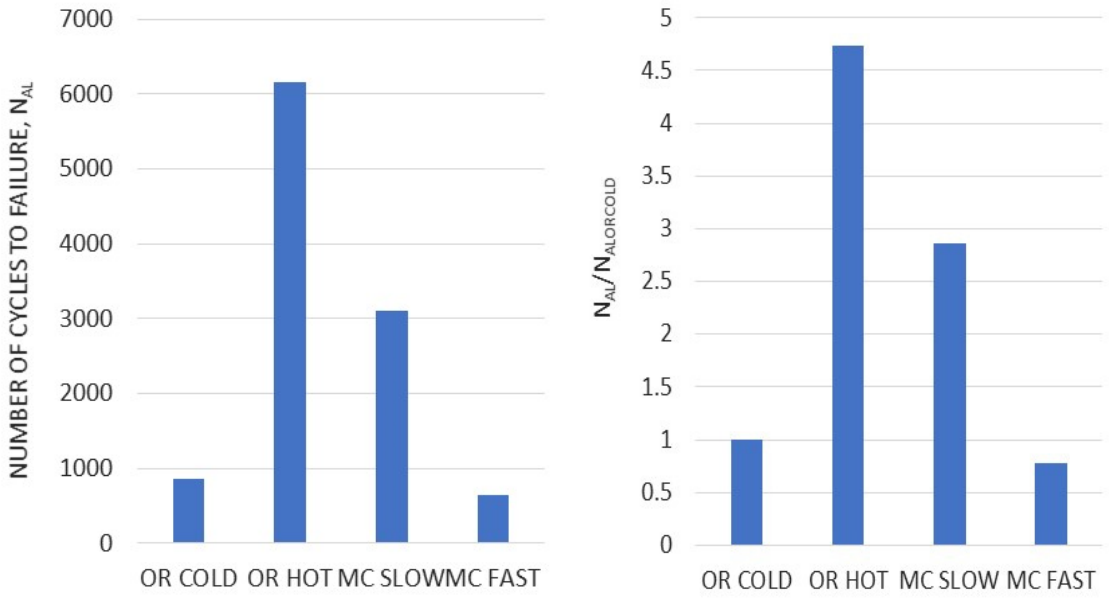

(**a**) (**b**)

Figure 16. The estimated fatigue life for each startup scenario, showing (**a**) the number of cycles to failure and (**b**) the ratios of fatigue lives.

Figure 16 shows the impact of the startup scenario on fatigue damage accumulation at a highly fatigued location on the drum. While the continued operation of the drum

after 250,000 h is possible, it should be noted that, following prolonged operation, the drum material may suffer greater fatigue deterioration at high temperature than at room temperature. The safety assessment of further operation requires a more precise analysis of the fatigue life of components, based on the changes in material properties following long-term operation.

By comparing the fatigue life of the used and unused specimens, it can be concluded that the former lost some amount of damage accumulation durability. Note, however, that this claim only applies to the crack initiation process.

The primary purpose of this analysis was to develop a method for estimating and comparing the fatigue life of a boiler drum under the various conditions that it may be subjected to. The analysis covers selected cases of mechanical and thermal loads, and identified a specific location on the internal surface of the drum as being highly susceptible to fatigue. However, this assessment method could be applied to any point within the drum, for which the stress and strain changes can be determined in simulation tests, and to the state of any material, the properties of which are subject to change throughout a period of use.

At this early stage of analysis, it is already clear that computer simulation methods are useful for estimating changes in mechanical states that occur under operating conditions. Computer simulation tools, combined with laboratory methods for assessing the durability of materials, can complement the diagnosis of energy equipment conditions, with particular reference to decisions regarding the continued operation of such equipment following prolonged use.

The results provided in this paper illustrate a method for determining physical fields within power components that are relevant for the occurrence of fatigue in areas of localized stress. More specifically, the current analysis presents a modelling approach that is necessary for the strength analysis of a boiler drum, in addition to methods for the estimation of local mechanical states and the subsequent prediction of the location and intensity of fatigue failure.

7. Conclusions

1. A combination of computer modeling and measurements under industrial conditions increases the accuracy of temperature field estimation, thereby improving the assessment of stress states as they relate to the current strength and fatigue life of pressure vessels in energy industries.
2. The impact of the startup procedure on the durability of power unit components can be assessed by analyzing changes in the physical fields of such units, which can be determined using a model-based approach.
3. The fatigue characteristics obtained in the low-cycle fatigue testing of used and unused specimens show a significant reduction in the room temperature material fatigue life of the former as compared to the latter.
4. The method for predicting fatigue life presented in this paper enables the superior estimation of the impact of mechanical and thermal loads on fatigue damage accumulation, and can be used to predict the effects of changes in the startup procedure.

Author Contributions: Conceptualization, J.O. and K.W.; methodology, J.O., G.J. and K.W.; validation, J.O., G.J. and M.T.; formal analysis, J.O. and K.W.; investigation, J.O., K.W., M.T. and G.J.; resources, M.T.; data curation, J.O., K.W. and G.J.; writing—original draft preparation, J.O.; writing—review and editing, J.O. and K.W.; visualization, J.O.; supervision, J.O.; project administration, K.W. All authors have read and agreed to the published version of the manuscript.

Funding: This research was funded by the National Centre for Research and Development under the project POIR.04.01.03-00-0001/17.

Data Availability Statement: Data are contained within the article.

Conflicts of Interest: The authors declare no conflict of interest.

References

1. *Standard EN 12952-3*; Water-Tube Boilers and Auxiliary Installations—Part 3: Design and Calculation for Pressure Parts. European Committee for Standardization: Brussels, Belgium, 2021.
2. Farragher, T.P.; Scully, S.; O'Dowd, N.P.; Leen, S.B. Development of life assessment procedures for power plant headers operated under flexible loading scenarios. *Int. J. Fatigue* **2013**, *49*, 50–61. [CrossRef]
3. Okrajni, J.; Twardawa, M. Local Strains That Lead to the Thermo-mechanical Fatigue of Thick-walled Pressure Vessels. *Mater. Perform. Charact. ASTM Int.* **2014**, *3*, 244–261. [CrossRef]
4. Farragher, T.P.; Scully, S.; O'Dowd, N.P.; Leen, S.B. Thermomechanical Analysis of a Pressurized Pipe Under Plant Conditions. *J. Press. Vessel Technol.* **2012**, *135*, 011204. [CrossRef]
5. Taler, J.; Dzierwa, P.; Jaremkiewicz, M.; Taler, D.; Kaczmarski, K.; Trojan, M.; Węglowski, B.; Sobota, T. Monitoring of transient 3D temperature distribution and thermal stress in pressure elements based on the wall temperature measurement. *J. Therm. Stress.* **2019**, *42*, 698–724. [CrossRef]
6. Banaszkiewicz, M. Online determination of transient thermal stresses in critical steam turbine components using a two-step algorithm. *J. Therm. Stress.* **2016**, *40*, 690–703. [CrossRef]
7. Banaszkiewicz, M. Numerical investigations of crack initiation in impulse steam turbine rotors subject to thermo-mechanical fatigue. *Appl. Therm. Eng.* **2018**, *138*, 761–773. [CrossRef]
8. Hahner, P.; Rinaldi, C.; Bicego, V.; Affeldt, E.; Brendel, T.; Andersson, H.; Beck, T.; Klingelhoffer, H.; Kuhn, H.J.; Koster, A.; et al. Research and development into a European code-of-practice for strain-controlled thermo-mechanical fatigue testing. *Int. J. Fatigue* **2008**, *30*, 371–381. [CrossRef]
9. Hormozi, R.; Biglari, F.; Nikbin, K. Experimental study of type 316 stainless steel failure under LCF/TMF loading conditions. *Int. J. Fatigue* **2015**, *75*, 153–169. [CrossRef]
10. Hormozi, R.; Biglari, F.; Nikbin, K. Experimental and numerical creep-atigue study of Type 316 stainless steel failure under high temperature LCF loading condition with different hold time. *Eng. Fract. Mech.* **2015**, *141*, 19–43. [CrossRef]
11. Hyde, C.J.; Sun, W.; Leen, S.B. Cyclil thermo-mechanical material modelling and testing of 316 stainless steel. *Int. J. Press. Vessels Pip.* **2010**, *87*, 365–372. [CrossRef]
12. Amiable, S.; Chapuliot, S.; Constantinescu, A.; Fissolo, A. A computational lifetime prediction of a thermal shock experiment. Part I: Thermomechanical modelling and lifetime prediction. *Fatigue Fract. Eng. Mater. Struct.* **2006**, *29*, 209–217. [CrossRef]
13. Pineau, A.; Antolovich, S.D. High temperature fatigue: Behaviour of three typical classes of structural materials. *Mater. High Temp.* **2015**, *32*, 298–317. [CrossRef]
14. Ji, D.M.; Shen, M.-H.H.; Wang, D.X.; Ren, J.X. Creep-Fatigue Life Prediction and Reliability Analysis of P91 Steel Based on Applied Mechanical Work Density. *J. Mater. Eng. Perform.* **2015**, *24*, 194–201. [CrossRef]
15. Nagesha, A.; Valsan, M.; Kannan, R.; Bhanu Sankara Rao, K.; Mannan, S.L. Influence of temperature on low cycle fatigue behaviour of a modified 9Cr-1Mo ferritic steel. *Int. J. Fatigue* **2002**, *24*, 1285–1293. [CrossRef]
16. Nagesha, A.; Kannan, R.; Sastry, G.; Sandhya, R.; Singh, V.; Rao, K.B.S.; Mathew, M. Isothermal and thermomechanical fatigue studies on a modified 9Cr-1Mo ferritic martensitic steel. *Mater. Sci. Eng. A* **2012**, *554*, 95–104. [CrossRef]
17. Nagesha, A.; Kannan, R.; Sandhya, R.; Sastry, G.; Mathew, M.; Rao, K.B.S.; Singh, V. Thermomechanical Fatigue Behaviour of a Modified 9Cr-1Mo Ferritic-Martensitic Steel. *Procedia Eng.* **2013**, *55*, 199–203. [CrossRef]
18. Wacławiak, K.; Okrajni, J. Transient heat transfer as a leading factor in fatigue of thick-walled elements of power boilers. *Arch. Thermodyn.* **2019**, *40*, 43–55. [CrossRef]
19. Okrajni, J.; Twardawa, M. Influence of a variable in time heat transfer coefficient on stresses in models of power plant components. *ASME J. Press. Vessel Technol.* **2014**, *136*, 041602. [CrossRef]
20. Pioro, I.L. Current status of research on heat transfer in forced convection of fluids at supercritical pressures. *Nucl. Eng. Des.* **2019**, *354*, 110–207. [CrossRef]
21. Mokry, S.; Pioro, I.; Farah, A.; King, K.; Gupta, S.; Peiman, W.; Kirillov, P. Development of supercritical water heat-transfer correlation for vertical baretubes. *Nucl. Eng. Des.* **2011**, *241*, 1126–1136. [CrossRef]
22. Jaromin, M.; Englart, H. A numerical study of heat transfer to supercritical water flowing upward invertical tubes under normal and deteriorated conditions. *Nucl. Eng. Des.* **2013**, *264*, 61–70. [CrossRef]
23. Jaremkiewicz, M.; Taler, J. Online Determining Heat Transfer Coefficient for Monitoring Transient Thermal Stresses. *Energies* **2020**, *13*, 704. [CrossRef]
24. Rudenko, A.G.; Voyevodin, V.N.; Gozhenko, S.V.; Mischenko, P.A. Studying the Metal from Drums at Thermal Power Plants after Long-Term Operation Using Subsize Charpy Specimens. *Therm. Eng.* **2021**, *68*, 640–646. [CrossRef]
25. Lepikhin, S.V.; Gladkovskii, S.V. The Influence of Low-Temperature Restorative Heat Treatment on the Structure and Mechanical Properties of Boiler Drum Metal after Long-Term Operation. *Therm. Eng.* **2020**, *67*, 138–1441. [CrossRef]
26. Ozhigov, L.S.; Mitrofanov, A.S.; Tolstolutskaya, G.D.; Vasilenko, R.L.; Rudenko, A.G.; Ruzhytskyi, V.V.; Ribalchenko, N.D.; Shramchenko, S.V. Comprehensive investigation of the metal in drums of boilers at thermal power stations. *Therm. Eng.* **2017**, *64*, 350–356. [CrossRef]
27. Radin, Y.A. Improving the Flexibility and Reliability of Steam Power Units at Thermal Power Plants. *Therm. Eng.* **2021**, *68*, 481–489. [CrossRef]

28. Drobenko, B.D. Computational experiment for determination of the cyclic durability of a boiler drum of a thermal power plant. *Mater. Sci.* **2012**, *48*, 76–82. [CrossRef]
29. Wacławski, A.; Bernacik, A.; Dobrzański, J.; Śniegoń, K.; Mandybur, K.; Miliński, P.; Doniec, B. Charakterystyki stali. In *Stale do Pracy w Temperaturach Podwyższonych*; Wydawnictwo Śląsk: Katowice, Poland, 1978.
30. Ansys. *Elements Reference, Release 11.0*; SAS IP, Inc.: Canonsburg, PA, USA, 2007.
31. Ansys. *Structural Analysis Guide, Release 12.1*; SAS IP, Inc.: Canonsburg, PA, USA, 2009.
32. Halama, R.; Sedlák, J.; Šofer, M. *Phenomenological Modelling of Cyclic Plasticity, Numerical Modelling*; Miidla, P., Ed.; InTech: London, UK, 2012; ISBN 978-953-51-0219-9.
33. Okrajni, J.; Twardawa, M.; Wacławiak, K. Impact of Heat Transfer on Transient Stress Fields in Power Plant Boiler Components. *Energies* **2021**, *14*, 862. [CrossRef]
34. Rusin, A.; Tomala, M.; Łukowicz, H.; Nowak, G.; Kosman, W. On-Line Control of Stresses in the Power Unit Pressure Elements Taking Account of Variable Heat Transfer Conditions. *Energies* **2021**, *14*, 4708. [CrossRef]
35. Huang, Z.; Wang, Z.; Zhu, S.; Yuan, F.; Wang, F. Thermomechanical fatigue behavior and life prediction of a cast nickel-based superalloy. *Mater. Sci. Eng. A* **2006**, *432*, 308–316. [CrossRef]
36. Meltzer, R.; Fiorini, Y.; Horstman, R.; Moore, I.; Batik, A.; Ostergren, W. A Damage Function and Associated Failure Equations for Predicting Hold Time and Frequency Effects in Elevated Temperature, Low Cycle Fatigue. *J. Test. Eval.* **1976**, *4*, 327. [CrossRef]
37. Okrajni, J.; Marek, A. The Attempt of the Low-Cycle Fatigue Life Description of Chosen Creep-Resistant Steels Under Mechanical and Thermal Interactions. *Arch. Met. Mater.* **2017**, *62*, 2349–2353. [CrossRef]